Experimental study on inertial hydrodynamic behaviors of a complex ROV

S.J. Xu[a], Q.W. Ma[b,a,*] and D.F. Han[a]

[a] College of Shipbuilding Engineering, Harbin Engineering University,

No.145 Nantong Street, 150001 Harbin, China

[b] School of Engineering and Mathematical, City University London,

Northampton Square, London, EC1V 0HB, UK

[*]Corresponding author: q.ma@city.ac.uk

ABSTRACT

This paper will present an experimental study on inertial hydrodynamic behaviors of an open-frame ROV (Remotely Operated Vehicle) that has a complex open-frame hull but has a large capacity holding more instruments on board than other ROVs. A 1:4 scaled model has been tested by a VPMM (vertical planar motion mechanism) in the circulating water channel of Harbin Engineering University. The inertial coefficients, which can be used for simulating the motions and so for predicting the maneuverability of the ROV, will be presented. Particular attention will be paid to discuss the properties of the cross inertial coefficients (these related to the inertial forces/moments induced by the motion in other directions).

Keywords: ROV (Remotely Operated Vehicle); inertial hydrodynamics coefficients; model tests; PMM (planar motion mechanism)

1. Introduction

There are increasing demands on underwater vehicles that can be used for inspection, repair and maintenance of marine/costal structures to ensure the safety of the structures, and for oceanic survey to explore and exploit ocean resources and to reveal the secrets in oceans. Generally, underwater vehicles may be divided into two types: Remotely Operated Vehicles

(ROVs) and Autonomous Underwater Vehicles (AUVs). In contrast to AUVs, which have simple and watertight hulls and are similar in many cases to conventional submarines, ROVs have relatively complex and open-frame hulls and their geometries can be very different from each other's. Therefore, it is more difficult to deal with the hydrodynamics of ROVs [1,2], and it may not be suitable to estimate their hydrodynamics coefficients of a new ROV from existing vehicles. In other words, one may have to consider their hydrodynamic properties on an individual basis.

The hydrodynamics of ROVs are important for controlling their motions and predicting their performance in the sea. There are three types of methods for quantifying the hydrodynamics of ROVs [1,2,3,4]: model test in a water tank by using the Planar Motion Mechanism (PMM), system identification (SI) and computational fluid dynamics (CFD). Model test method with PMM is the most traditional method and is suitable for vehicles with complex geometric hulls and may allow to evaluate all hydrodynamics more accurately, depending on availability of laboratory facilities and instruments. System identification (SI) method is that data are gathered by free-running trials of a ROV and hydrodynamic forces are estimated by using the data measured during the trials in a water tank [10] or in a real water area such as a lake or reservoir. This method requires a vehicle that is equipped with all components (such as propellers and thrusters) for the free-running trials of a model or even prototype in addition to on-board sensors. Theoretically, computational fluid dynamics (CFD) is able to simulate all model tests. However, for the vehicles like ROVs with complex hull geometries, it may be very time-consuming and not easy to resolve the flow fields around small scale structural members. In addition, the existing CFD methods are rarely validated for flow associated with such complex structures and so its effectiveness on modelling the flow concerned has yet be confirmed. This paper is concerned about using the model test with the Planar Motion Mechanism (PMM) to study the inertial hydrodynamic property of a ROV.

There have been a limited number of publications that deal with inertial hydrodynamic of different ROVs. Avila et al [8,9,10] carried out a series of study with system identification method as well as model test method with PMM to estimate inertial and drag hydrodynamic components based on the Morison's equation for a ROV composed mainly of cylinders and

jacket-type structural members. They only considered the main inertial coefficients (related to the inertial hydrodynamic forces generated by a motion in the same direction) without counting for the cross inertial coefficients (related to the inertial hydrodynamic forces generated by a motion in other directions). Nomoto et al [11] studied the inertial properties and motions of a ROV composed mainly of the pipes and buoyant blocks. They just assumed the cross inertial oefficients equal to each other when processing their data, and found they were negligible. Fan et al [12] presented a series of model tests to identify inertial and drag coefficients of a ROV composed mainly of a top box and small blocks/cylindrical structural members. They demonstrated that the cross inertial coefficients might not be the same, though their values would be relatively small. Eng et al [13] discussed a novel free decay test to determine the hydrodynamic coefficients for a ROV composed mainly of rocket-type cylinders. They compared numerical and experimental results but did not consider the cross inertial forces/moments. In addition, there are also some studies based on numerical computations. For examples, Lin et al [6] applied the fast multiple boundary element method (FMBEM) to calculate the inertial coefficients of a submarine. Paper [14] proposed a method to determine the inertial coefficients by using WAMIT that is based on the velocity potential theory. Yang et al [15] modeled an underwater vehicle and estimated the inertial coefficients again by using WAMIT but estimated damping parameters corresponding to constant velocities by using CFD. Although this paper made some attempts to validate the CFD results, the CFD method needs further validation to ensure that its results are reliable, as indicated above.

In order to investigate the relative importance of the cross inertial confidents and to provide experimental data to be used perhaps for validating numerical methods, this paper will present an experimental study on a ROV with a complex asymmetrical shape, similar to the Quantum designed by SMD [16]. This ROV has better capacity for heavy duties, and has a complex open-framed hull with its front-rear and top-bottom asymmetry, which is quite different from those ROV discussed in the cited papers above. Xu et al [19] presented the experimental results for the drag forces and moments of this ROV subjected to constant velocities, which are measured by holding the models in water flowing with a constant speed or towing the

model with a constant speed in water at rest. In this paper, the authors will focus on its inertial hydrodynamic forces and moments on the model. These forces and moments are measured by oscillating the model with a time-dependent acceleration. As the nature of inertial hydrodynamics is different from that of the drag forces and moments, the processing method of experimental data employed here is different from that used in Xu et al [19]. It is hoped that the data given in the paper can contribute to the pool of knowledge about underwater vehicles.

The remainder of this paper is organized as follows. In Section 2, the test model, experimental facilities as well as procedure will be summarized. Section 3 presents the data processing method. Then the experimental results are given and discussed in Section 4. Finally, the conclusions are summarized in Section 5.

2. Test model, experimental facilities and procedures

The test model of the vehicle is illustrated in Fig 1. The frame structure is made of steel, while the other components within the frame, such as thrusters and equipment blocks are made of buoyancy material. Its main parameters are summarized in Table 1. The test model is front-rear and top-bottom asymmetrical. Fig. 2 shows its longitudinal section at the middle of its width and the transverse section at a positon of 0.498m from the head of test model. The information has been given in [19].

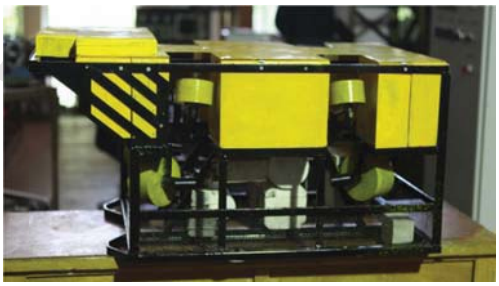

Fig 1 Test model

Table 1

Parameters of test model

Physical property	Value
Scale ratio	1:4
length, m	0.875
width, m	0.5
height, m	0.5
mass in air, kg	78

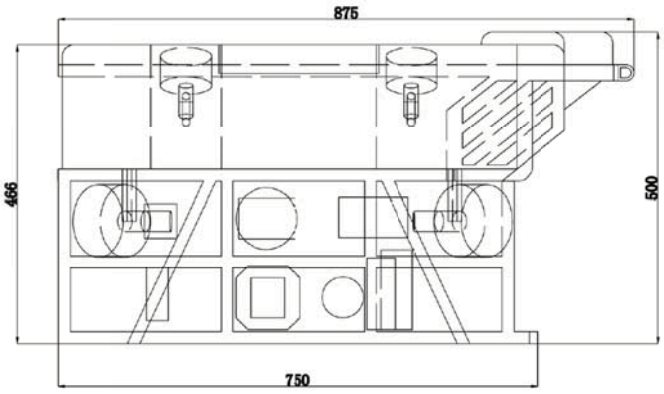

(a) The longitudinal section of test model at the middle of its width

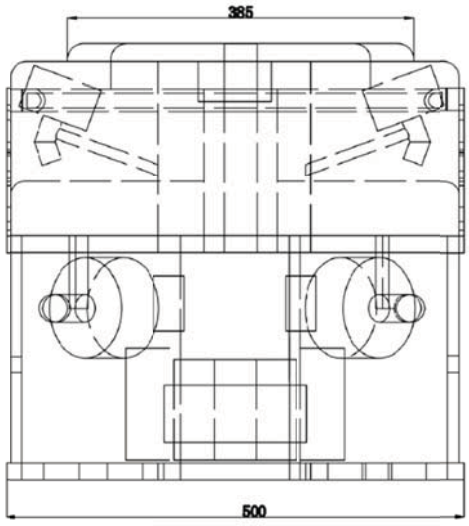

(b) The transverse section of test model at a positon of 0.498m from the head of test model

Fig 2 The sectional view of test model

For the sake of studying the inertia hydrodynamic behaviors of the vehicle, a series of forced oscillation tests have been carried out, that is purely heaving test, purely swaying test, purely pitching test and purely yawing test, respectively. All these tests have been undertaken in a circulating water channel with the help of a vertical planar motion mechanism (VPMM). The water channel has a cross-section of 1.7m wide and 1.5m deep with the constant velocity of water flow. The VPMM has the maximum oscillation amplitude of 0.04 m and the oscillation frequency from 0.05Hz to 1Hz. The forces and moments acting on the test model are measured by the use of a six-component force transducer, which is fixed inside the ROV model and connected by two steel bars to the VPMM. One end of each bar is fixed with the force transducer and the other end extends out of water to be fixed with the two rotating apparatus of the VPMM (as shown in Fig 3). Before test starts, the model is submerged in water and its gravity force is adjusted equals to its buoyancy. During tests, the model is forced through the bars to oscillate together with the VPMM, while the water in the circulating water channel flows at a constant speed. When the two bars move with the same phases, frequencies and amplitudes, the purely heaving and swaying tests can be undertaken, while when the bars move with the same frequencies and amplitudes but different phases, the purely pitching and yawing tests can be done. Fig 4 shows a status during a purely heaving test.

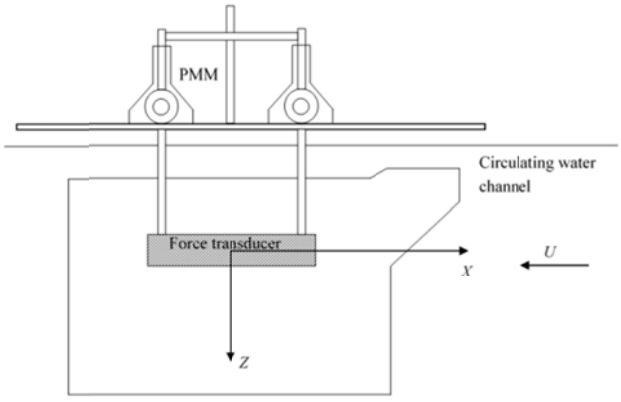

Fig 3 The installation of ROV model

Fig 4 Model test in circulating water channel

3. Data processing methods

This section will discuss how the experimental data are analyzed and what the data processing methods are. As a result, the expressions for the inertial forces and moments will be given.

3.1 Expressions of inertial forces and moments

In order to describe forces, moments and motions of the test model more conveniently, the coordinate systems are set up as shown in Fig 5. *G-xyz* represents the body-fixed coordinate system of the ROV model with the center of gravity *G* at its origin. Vector $\boldsymbol{X} \in \mathbb{R}^3$ $(\boldsymbol{X} = [x\ y\ z]^T)$ and $\boldsymbol{\Theta} \in \mathbb{R}^3$ $(\boldsymbol{\Theta} = [\varphi\ \theta\ \psi]^T)$ represent the motions in surge, sway, heave or roll, pitch, yaw directions respectively. While, vector $\boldsymbol{v} \in \mathbb{R}^6$ $(\boldsymbol{v} = [u\ v\ w\ p\ q\ r]^T)$ as well as $F \in \mathbb{R}^6$ $\boldsymbol{F} = [X\ Y\ Z\ K\ M\ N]^T$ denote corresponding linear or angular velocities as well as forces or moments acted on the ROV model in the body-fixed system. A dot above the parameters, such as $\dot{w}$, denotes their time derivatives. *E-ξηζ* is the earth-fixed coordinate system. The position of *G* with respect to the earth-fixed frame (*E-ξηζ*) can be expressed by a position vector $\boldsymbol{p} \in \mathbb{R}^3$ $(\boldsymbol{p} = [\xi\ \eta\ \zeta]^T)$, while the orientation of the body-fixed frame (*E-ξηζ*) with respect to the earth-fixed system (*E-ξηζ*) is represented by using $\boldsymbol{\Theta} \in \mathbb{R}^3$.

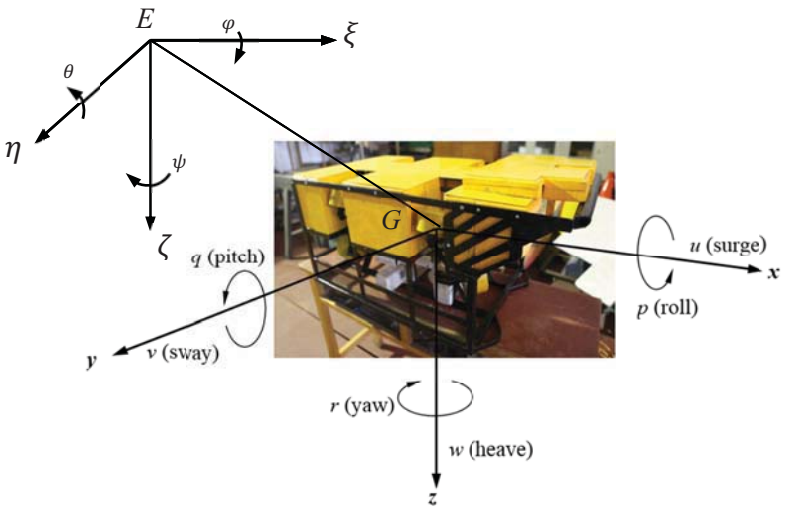

Fig 5 Coordinate system and illustration of motions

According to [17], the motion equations of a vehicle with respect to the body-fixed system can be written as:

$$\boldsymbol{F}_t = M\dot{\boldsymbol{v}} + C(\boldsymbol{v})\boldsymbol{v} - \boldsymbol{F_R}(\boldsymbol{\Theta}) - \boldsymbol{F_I}(\dot{\boldsymbol{v}}) - \boldsymbol{F_D}(\boldsymbol{v}) \tag{1}$$

where, $\boldsymbol{F}_t$ represents total forces and moments acting on ROV model during tests through the force transducer; $M \in \mathbb{R}^{6\times6}$ represents its inertial matrix, including mass and moments of inertia; $C(\boldsymbol{v}) \in \mathbb{R}^{6\times6}$ is Coriolis matrix; $\boldsymbol{F_R}$, $\boldsymbol{F_I}$ and $\boldsymbol{F_D} \in \mathbb{R}^6$ denote its restore, inertia and damping forces and moments vectors. Considering that the model is left-right symmetric, the matrixes of M and C can be expressed as [17,18]

$$M = \begin{bmatrix} m & 0 & 0 & 0 & 0 & 0 \\ 0 & m & 0 & 0 & 0 & 0 \\ 0 & 0 & m & 0 & 0 & 0 \\ 0 & 0 & 0 & I_x & 0 & -I_{xz} \\ 0 & 0 & 0 & 0 & I_y & 0 \\ 0 & 0 & 0 & -I_{xz} & 0 & I_z \end{bmatrix} \tag{2}$$

$$C(\boldsymbol{v}) = \begin{bmatrix} 0 & 0 & 0 & 0 & mw & -mv \\ 0 & 0 & 0 & -mw & 0 & mu \\ 0 & 0 & 0 & mv & -mu & 0 \\ 0 & mw & -mv & 0 & -I_{xz}p + I_z r & -I_y q \\ -mw & 0 & mu & I_{xz}p - I_z r & 0 & -I_{xz}r + I_x p \\ mv & -mu & 0 & I_y q & I_{xz}r - I_x p & 0 \end{bmatrix} \tag{3}$$

Suppose that W and B are the model's gravity and buoyancy, and as discussed in the last section, the model's gravity is equal to its buoyancy, i.e. $W = B = mg$. In addition, the position of $G\,(x_G, y_G, z_G)$ is at the origin of the body-fixed system, and so $x_G = y_G = z_G = 0$. As its left-right symmetry, the positon of the buoyancy center with respect to the body-fixed system is in the longitudinal plane and so $x_B = y_B = 0$. Therefore, $\boldsymbol{F_R}$ is reduced [17] to

$$\boldsymbol{F_R} = \begin{bmatrix} (W-B)\sin\theta \\ -(W-B)\cos\theta\sin\varphi \\ -(W-B)\cos\theta\cos\varphi \\ -(y_G W - y_B B)\cos\theta\cos\varphi + (z_G W - z_B B)\cos\theta\sin\varphi \\ (z_G W - z_B B)\sin\theta + (x_G W - x_B B)\cos\theta\cos\varphi \\ -(x_G W - x_B B)\cos\theta\sin\varphi - (y_G W - y_B B)\sin\theta \end{bmatrix} = -mgz_B \begin{bmatrix} 0 \\ 0 \\ 0 \\ \cos\theta\sin\varphi \\ \sin\theta \\ 0 \end{bmatrix} \tag{4}$$

As well known, the magnitudes of inertial forces and moments are proportional to acceleration vector $\dot{\boldsymbol{v}}$, i.e., $\boldsymbol{F_I}(\dot{\boldsymbol{v}}) = M_A\dot{\boldsymbol{v}}$, where $M_A \in \mathbb{R}^{\boldsymbol{6\times 6}}$ represents inertia coefficients matrix. Considering the left-right symmetry of ROV, the inertia forces and moments of the model [17] can be reduced to

$$\boldsymbol{F_I}(\dot{\boldsymbol{v}}) = M_A\dot{\boldsymbol{v}} = \begin{bmatrix} X_{\dot{u}} & 0 & X_{\dot{w}} & 0 & X_{\dot{q}} & 0 \\ 0 & Y_{\dot{v}} & 0 & Y_{\dot{p}} & 0 & Y_{\dot{r}} \\ Z_{\dot{u}} & 0 & Z_{\dot{w}} & 0 & Z_{\dot{q}} & 0 \\ 0 & K_{\dot{v}} & 0 & K_{\dot{p}} & 0 & K_{\dot{r}} \\ M_{\dot{u}} & 0 & M_{\dot{w}} & 0 & M_{\dot{q}} & 0 \\ 0 & N_{\dot{v}} & 0 & N_{\dot{p}} & 0 & N_{\dot{r}} \end{bmatrix} \begin{bmatrix} \dot{u} \\ \dot{v} \\ \dot{w} \\ \dot{p} \\ \dot{q} \\ \dot{r} \end{bmatrix} \tag{5}$$

where $X_{\dot{u}}$ denotes the coefficient of the inertial force in x-direction due to the motion in the x-direction, and others have similar meaning. The diagonal coefficients are referred to the main coefficients whereas the off-diagonal coefficients are to the cross inertial coefficients in this paper.

The damping force and moment matrixes $\boldsymbol{F_D}$ are known to be a function of velocities. Generally, the components of damping forces and moments can be expressed by the multivariate Taylor series in terms of the velocities [17]. However, the magnitudes of the oscillation velocities are small during oscillation tests and so it is reasonable to take the series to the first order and ignore the asymmetry of damping hydrodynamic forces and moments caused by the asymmetrical model shape, according to what is discussed in [19]. In other words, it is here assumed that all damping hydrodynamic forces and moments acting on the ROV model during oscillation tests are linear and can be written as

$$\boldsymbol{F_D}(u, V) = \boldsymbol{F}_u u + \boldsymbol{F}_V V \tag{6}$$

where u is the constant velocity in the direction concerned and V represents the oscillation velocity of *w, v, q, r* corresponding to oscillation tests in heave, sway, pitch and yaw directions, respectively. Specifically, the expressions for the damping forces and moments for different model tests are given by

$F_D = F_u u + F_w w$ (for $F_D = X_D, Z_D, M_D$); $F_D = 0$ (for $F_D = Y_D, K_D, N_D$) for purely heaving test (7)

$F_D = F_u u$ (for $\mathrm{F_D} = X_D, Z_D, M_D$); $F_D = F_v v$ (for $F_D = Y_D, K_D, N_D$) for purely swaying test (8)

$F_D = F_u u + F_q q$ (for $F_D = X_D, Z_D, M_D$); $F_D = 0$ (for $F_D = Y_D, K_D, N_D$) for purely pitching test (9)

$F_D = F_u u$ (for $F_D = X_D, Z_D, M_D$); $F_D = F_r r$ (for $F_D = Y_D, K_D, N_D$) for purely yawing test (10)

where F_u is the coefficient of the damping forces in x-direction related to u, and others have the similar meaning. Substituting Eqs. (2-5) and Eqs. (7-10) into Eq. (1), the total forces and moments measured by the force transducer during oscillation tests can be written as the following forms.

Purely heaving test:

$$X_t = -X_{\dot{w}}\dot{w} - X_u u - X_w w; \tag{11a}$$

$$Z_t = (m - Z_{\dot{w}})\dot{w} - Z_u u - Z_w w; \tag{11b}$$

$$M_t = -M_{\dot{w}}\dot{w} - M_u u - M_w w; \tag{11c}$$

Purely swaying test:

$$Y_t = (m - Y_{\dot{v}})\dot{v} - Y_v v; \tag{12a}$$

$$K_t = -K_{\dot{v}}\dot{v} - K_v v; \tag{12b}$$

$$N_t = -N_{\dot{v}}\dot{v} - N_v v \tag{12c}$$

Purely pitching test:

$$X_t = -X_{\dot{q}}\dot{q} - X_u u - X_q q; \tag{13a}$$

$$Z_t = -muq - Z_{\dot{q}}\dot{q} - Z_u u - Z_q q; \tag{13b}$$

$$M_t = \left(I_y - M_{\dot{q}}\right)\dot{q} + mgz_B \sin\theta - M_u u - M_q q \tag{13c}$$

Purely yawing test:

$$Y_t = mur - Y_{\dot{r}}\dot{r} - Y_r r; \tag{14a}$$

$$K_t = -K_{\dot{r}}\dot{r} - K_r r; \tag{14b}$$

$$N_t = (I_z - N_{\dot{r}})\dot{r} - N_r r \tag{14c}$$

3.2 Parameter Identification Methods

Inertial coefficients can be obtained by two approaches, although both of them are based on the ordinary Least Squared Method. Specifically, one approach directly uses the Least Squared Method to fit the measured total forces and moments into Eqs. (11-14). This method enables us to use the measured data directly. In the other approach, the inertial parts are separated from the total measured results firstly, and then uses the Least Squared Method to only fit inertial coefficients. The direct use of the Least Squared Method (i.e., the 1st approach) is similar in principle to what has been discussed in our previous paper (Xu et al [19]) for analyzing the drag forces and moments corresponding to motions with constant velocities. The main difference is that the equations for fitting used here are these including the accelerations as given in Eqs. (11)-(14), rather than those equations in terms of only constant velocities in [19]. The basic theory of the least square method is the same and so more details will not be given here. The discussion about the second approach will be given below.

Specifically, for purely heaving and swaying tests, the ROV model is forced to oscillate with a amplitude (A) and frequency (f) in the channel while water with a constant speed flows toward the model. Therefore, the motions are expressed by:

$$\begin{cases} u = U \\ S = Asin\omega t \\ V = \dot{S} = \omega Acos\omega t = V_0 cos\omega t \\ \dot{V} = \ddot{S} = -\omega^2 Asin\omega t = -\dot{V}_0 sin\omega t \end{cases} \tag{15}$$

where ω represents the angular frequency, $\omega = 2\pi f$; S is the oscillating displacement in heave or sway direction; V and $\dot{V}$ are the corresponding velocity and acceleration, $V = w$ or v, $\dot{V} = \dot{w}$ or $\dot{v}$; V_0 and $\dot{V}_0$ represents the amplitudes of corresponding velocity and acceleration, $V_0 = w_0$ or v_0, $\dot{V}_0 = \dot{w}_0$ or $\dot{v}_0$.

According to Eq. 3 and Eq. (4), $C(\boldsymbol{v})\boldsymbol{v} = \boldsymbol{0}$ and $\boldsymbol{F_R} = \boldsymbol{0}$ for these tests. Consequently, forces and moments in Eq. (1) specifically for purely heaving and swaying tests can be rewritten as:

$$\begin{aligned} \boldsymbol{F}_t(u,V) &= (M - M_A)\dot{V} - \boldsymbol{F}_V V - \boldsymbol{F}_u U \\ &= -(M - M_A)\dot{V}_0 sin\omega t - \boldsymbol{F}_V V_0 cos\omega t - \boldsymbol{F}_u U \\ &= \boldsymbol{F}_s sin\omega t - \boldsymbol{F}_c cos\omega t - \boldsymbol{F}_0(U) \end{aligned} \tag{16}$$

As can be seen in the equation above, total forces and moments $\boldsymbol{F}_t$ can be divided into 3 parts: the part only associated with $sin\omega t$, i.e. $\boldsymbol{F}_s sin\omega t$; the part only with $cos\omega t$, i.e. $\boldsymbol{F}_c cos\omega t$ and the part without oscillation, i.e. $\boldsymbol{F}_0$. Based on this, one can identify the inertia force amplitudes $\boldsymbol{F}_s$ by applying the following integrations

$$\boldsymbol{I}_1 = -\frac{1}{2n\pi}\int_0^{2n\pi} \boldsymbol{F}_t \, d\omega t = \boldsymbol{F}_0 \tag{17}$$

$$\boldsymbol{I}_2 = \frac{1}{2n\pi}\int_0^{2n\pi} (\boldsymbol{F}_t - \boldsymbol{F}_0) sin\omega t \, d\omega t = \boldsymbol{F}_s \tag{18}$$

where *n* is the number of periods of motions recorded, excluding the initial transient periods.

For purely pitching and yawing tests, the motions are given as follows:

$$\begin{cases} u = U \\ \phi = \phi_0 sin\omega t \\ \Omega = \dot{\phi} = \omega\phi_0 cos\omega t = \Omega_0 cos\omega t \\ \dot{\Omega} = \ddot{\phi} = -\omega^2\phi_0 sin\omega t = -\dot{\Omega}_0 sin\omega t \end{cases} \tag{19}$$

where Ω and $\dot{\Omega}$ are the corresponding angular velocity and acceleration, $\Omega = q$ or r, $\dot{\Omega} = \dot{q}$ or $\dot{r}$; Ω_0 and $\dot{\Omega}_0$ represents the amplitudes of corresponding angular velocity and acceleration, $\Omega_0 = q_0$ or r_0, $\dot{\Omega}_0 = \dot{q}_0$ or $\dot{r}_0$. During purely pitching and yawing tests, the oscillation angles all have small values, F_R in Eq. (4) can be reduced to $\boldsymbol{F_R} = [0, 0, 0, 0, -mg\, z_B \sin\phi,\ 0]^T \approx [0, 0, 0, 0, -mgz_B\phi, 0]^T = [0, 0, 0, 0, -mgz_B\phi_0 sin\omega t, 0]^T$ for purely pitching motion, while $\boldsymbol{F_R}$ is zero for purely yawing motion. According to Eq.(3), $C(\boldsymbol{v})\boldsymbol{v} = C(u)\Omega$ and the value of $C(u)$ does not change. Consequently, total forces and moments can also be rewritten as the same form as Eq. (16), and so the inertial part can be identified in the same way described above. After identifying and evaluating $\boldsymbol{F}_s$, the inertia force and moment coefficients can be obtained by fitting the measured data as given below for each test.

$$X_s = X_{\dot{w}}\dot{w}_0,\ Z_s = (Z_{\dot{w}} - m)\dot{w}_0,\ M_s = M_{\dot{w}}\dot{w}_0,\ \text{others are zero for purely heaving test} \tag{20}$$

$Y_s = (Y_{\dot{v}} - m)\dot{v}_0$, $K_s = K_{\dot{v}}\dot{v}_0$, $N_s = N_{\dot{v}}\dot{v}_0$, others are zero for purely swaying test (21)

$X_s = X_{\dot{q}}\dot{q}_0$, $Z_s = Z_{\dot{q}}\dot{q}_0$, $M_s = \left(M_{\dot{q}} - I_y\right)\dot{q}_0 + mgz_B\phi_0$, others are zero for purely pitching test (22)

$Y_s = Y_{\dot{r}}\dot{r}_0$, $K_s = K_{\dot{r}}\dot{r}_0$, $N_s = (N_{\dot{r}} - I_z)\dot{r}_0$, others are zero for purely yawing test (23)

4. Results and discussions

In this section, the experimental results as well as corresponding coefficients are presented and discussed firstly. Then the comparison between inertial cross inertial coefficients are given together with relevant discussions. As pointed above, a series of forced oscillation tests have been undertaken in heave, sway, pitch and yaw directions, respectively, with varying frequencies and flow velocities in the circulating water channel. During these tests, the water flow velocities in the channel are set to be 0.5m/s and 0.7m/s while their real values are measured to be 0.532m/s and 0.751m/s, respectively. The test model is forced to oscillate with different frequencies from 0.1Hz to 0.5Hz. The oscillation amplitude for heaving and swaying tests is 0.02m, while those for pitching and yawing are at a range of 0.023 rad to 0.073 rad.

4.1 Experimental results for different tests

The results for heaving tests are considered at first. During the heaving tests, it is found that the amplitudes of the vertical inertial force Z_s and pitch inertial moment M_s are much larger than the inertial forces and moments in other directions. For an example, the maximum magnitude of the inertial surge force X_s is less than 0.5N while that of Z_s is more than 25N. Based on this fact, only Z_s and M_s obtained given by Eqs. (17-18) are presented in Fig. 6, where $Z'_s = Z_s/\frac{1}{2}\rho l^2 w_0$, $M'_s = M_s/\frac{1}{2}\rho l^3 w_0$, with ρ, l and w_0 representing the water density, the model length and the amplitude of oscillation velocity, respectively. These on the left in the figure show the dimensionless amplitudes of inertial forces or moments against the

oscillation frequency, while these on the right give the corresponding dimensional amplitudes against the acceleration amplitudes. First of all, as depicted on the left column in Fig 6, the dimensionless amplitudes of the inertial forces Z'_s and moments M'_s increase largely in a linear way with the increase of frequency. Secondly, the dimensional amplitudes of the inertial forces or moments on the right column decrease largely in a linear way with the increase of acceleration amplitudes. They are consistent with each other as the dimensionless amplitudes are obtained by dividing a term of ωA (i.e., the velocity amplitude).

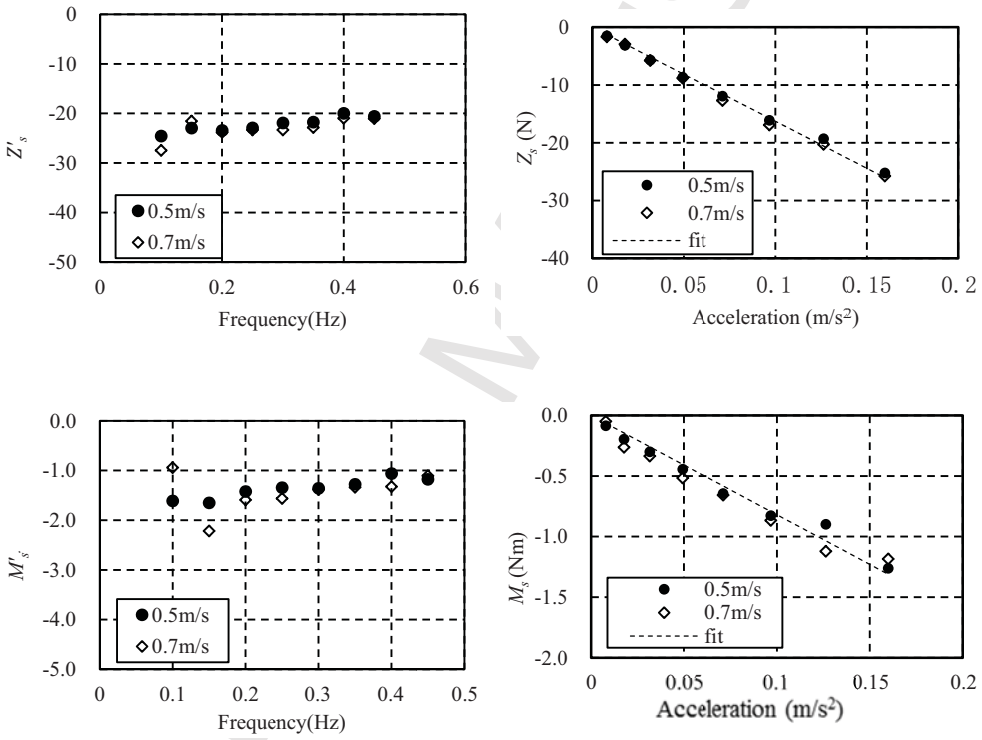

Fig 6 Inertial force and moment for purely heaving test (acceleration = $A\omega^2$)

Table 2 inertial coefficients for heaving tests

set flow velocity (m/s)	real flow velocity (m/s)	$Z_{\dot{w}}$ (kg)	$M_{\dot{w}}$ (kg·m)	$Z'_{\dot{w}}$ $(Z'_{\dot{w}} = Z_{\dot{w}}/\frac{1}{2}\rho l^3)$	$M'_{\dot{w}} \times 10^2$ $(M''_{\dot{w}} = M_{\dot{w}}/\frac{1}{2}\rho l^4)$
0.5	0.532	-86.7	-7.98	-0.259	-2.72

		(-87.5)	(-8.41)	(-0.261)	(-2.87)
0.7	0.751	-92.6 (-93.1)	-8.42 (-8.95)	-0.277 (-0.278)	-2.87 (-3.05)
average		-89.7 (-90.3)	-8.20 (-8.68)	-0.268 (-0.269)	-2.80 (-2.96)

The measured data on the right column of Fig. 6 can be fitted by using the second approach based on Eq. (20) or the first approach based on Eq. (11) to give the inertial coefficients ($Z_{\dot{w}}$, $M_{\dot{w}}$). The resulting values for two velocities obtained by using the two approaches are all shown in Table 2, where the dimensionless forms of the coefficients are also presented. The corresponding values in brackets are obtained by the first approach. One can see that the difference between the corresponding values of two velocities of water in the circulating channel are less than 10%. On this basis, the mean values over the two velocities may be utilized. Based on the mean values, the fitting curves from Eq. (20) are also plotted in Fig. 6. As one can see, the fitting curves agree well with the measured data.

As observed from Table 2, the inertial coefficients obtained by the two approaches are very close to each other. More specially, the largest difference occurs in estimating the inertial coefficients of $M_{\dot{w}}$ for the velocity of 0.751 m/s, i.e., $M_{\dot{w}} \approx -8.95$ kg.m estimated by the first approach while $M_{\dot{w}} \approx -8.42$ kg.m by the second approach, with the relative error being less than 6.3%. The average inertial coefficients of $Z_{\dot{w}}$ from the two approaches are almost the same. The average inertial coefficients of $M_{\dot{w}}$ is -8.20 and -8.68 kg.m estimated by the second and first approach, respectively, yielding the relative error of less than 6%. The level of the error is believed to be similar to that of the experimental facilities and process, as indicated in Xu et al [19]. Therefore, the results from the first approach will not, hereafter, be discussed as they do not provide more useful information.

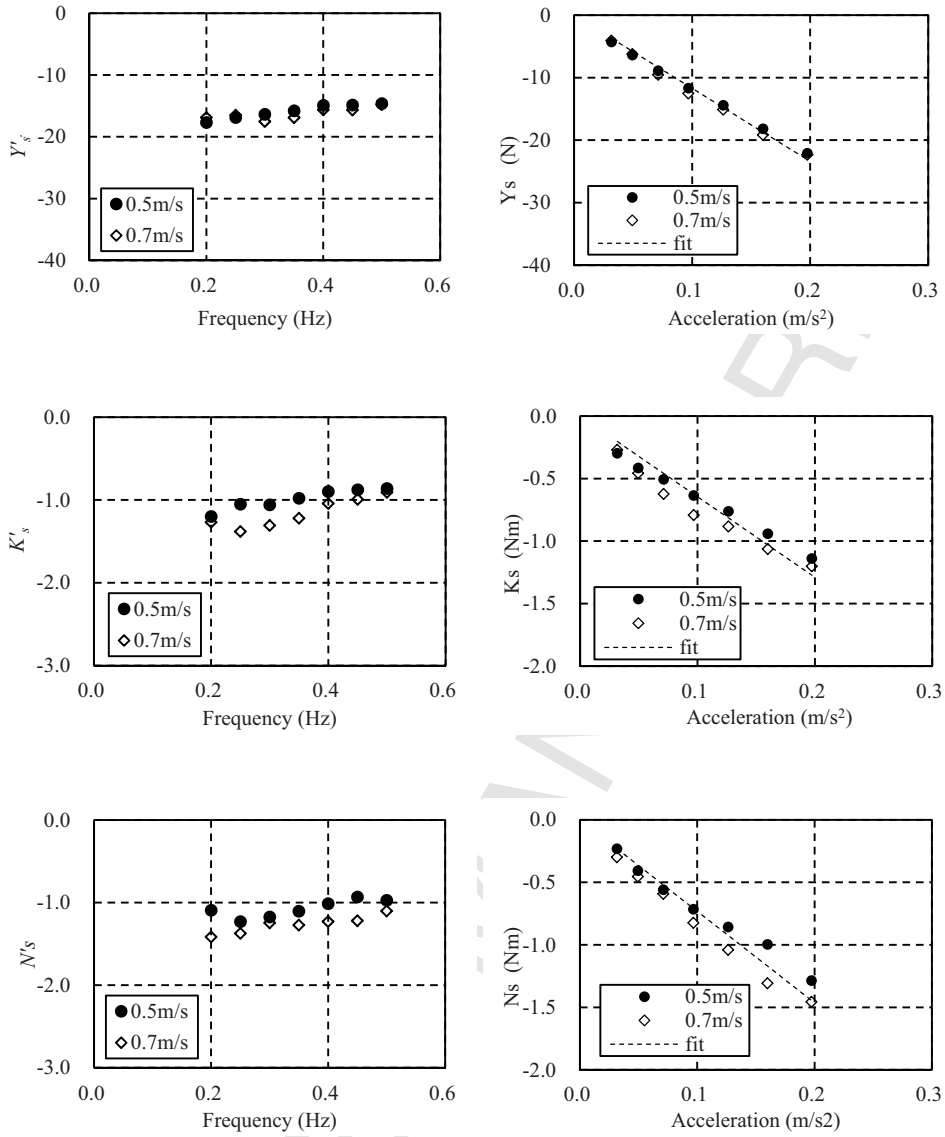

Fig 7 Inertial force and moment for purely swaying test (acceleration = $A\omega^2$)

Experimental results obtained by using Eqs. (17-18) for purely swaying tests are depicted in Fig 7, where $Y'_s = Y_s/\frac{1}{2}\rho l^2 v_0$; $K'_s = K_s/\frac{1}{2}\rho l^3 v_0$; $N'_s = N_s/\frac{1}{2}\rho l^3 v_0$. Similar to those in Fig.6, these on the left column are the dimensionless amplitudes of the inertial forces or moments against oscillation frequency, while these on the right are the corresponding dimensional results plotted against the acceleration amplitudes. The behaviors of the inertial forces and moments are similar to these shown in Fig. 6, i.e., they linearly vary with changes of acceleration amplitudes. Compared with the vertical inertial forces in the heaving tests, the horizontal inertial forces in the y-direction are in the same order, though they are slight smaller here. The inertial moments induced by swaying are also in the same order as those in the heaving

tests. These measured data denoted by the symbols in Fig. 7 are fitted by Eq. (21). The corresponding coefficients are given in Table 3. Using the mean coefficients in the last row of Table 3 and Eq. (21), the fitting curves (dotted lines) for each of inertial forces and moments are also shown in Fig. 7. The agreement between the measure data and fitting curves are acceptable, though there are some visible difference (about 5%) in the roll and yaw moments (K_s and N_s). Such difference may be considered as insignificant for practical purpose.

Table 3 Inertial coefficients for swaying test

set flow velocity (m/s)	real flow velocity (m/s)	$Y_{\dot{v}}$ (kg)	$K_{\dot{v}}$ (kg·m)	$N_{\dot{v}}$ (kg·m)	$Y'_{\dot{v}}$ $\left(Y'_{\dot{v}} = Y_{\dot{v}}/\frac{1}{2}\rho l^3\right)$	$K'_{\dot{v}} \times 10^2$ $\left(K'_{\dot{v}} = K_{\dot{v}}/\frac{1}{2}\rho l^4\right)$	$N'_{\dot{v}} \times 10^2$ $\left(N'_{\dot{v}} = N_{\dot{v}}/\frac{1}{2}\rho l^4\right)$
0.5	0.532	-41.9	-6.08	-6.69	-0.125	-2.08	-2.28
0.7	0.751	-45.9	-6.82	-7.95	-0.137	-2.33	-2.71
average		-43.9	-6.45	-7.32	-0.131	-2.20	-2.50

Fig 8 and Fig 9 plot inertial force and moment amplitudes resulting from purely pitching and yawing tests respectively, where, $Z'_s = Z_s/\frac{1}{2}\rho l^4 q_0$; $M'_s = M_s/\frac{1}{2}\rho l^5 q_0$; $Y'_s = Y_s/\frac{1}{2}\rho l^4 r_0$; $N'_s = N_s/\frac{1}{2}\rho l^5 r_0$ with other parameters same as defined before. As in previous figures, the dimensionless amplitudes are shown in the left column whereas the dimensional ones on the right. Because other components are relatively very small, only the vertical inertial force Z and the pitch inertial moment *M* in purely pitching tests and the lateral inertial force *Y* and yaw inertial moment N in purely yawing tests are presented in the figures. As can be seen, the linearity between the inertial forces (moments) and the acceleration amplitudes still hold. In addition, the magnitudes of the corresponding inertial forces and moments from pitching and yawing tests are also in the same order as has been seen for the heaving and swaying tests. The corresponding inertial coefficients ($Z_{\dot{q}}$,$M_{\dot{q}}$) and ($Y_{\dot{r}}$,$N_{\dot{r}}$) fitted by Eq. (22) and (23), respectively, are given in Table 4. The fitting curves based on the average values of the coefficients are plotted in Fig. 8 and Fig. 9. Again the agreement between the fitting results and the measure data are very good.

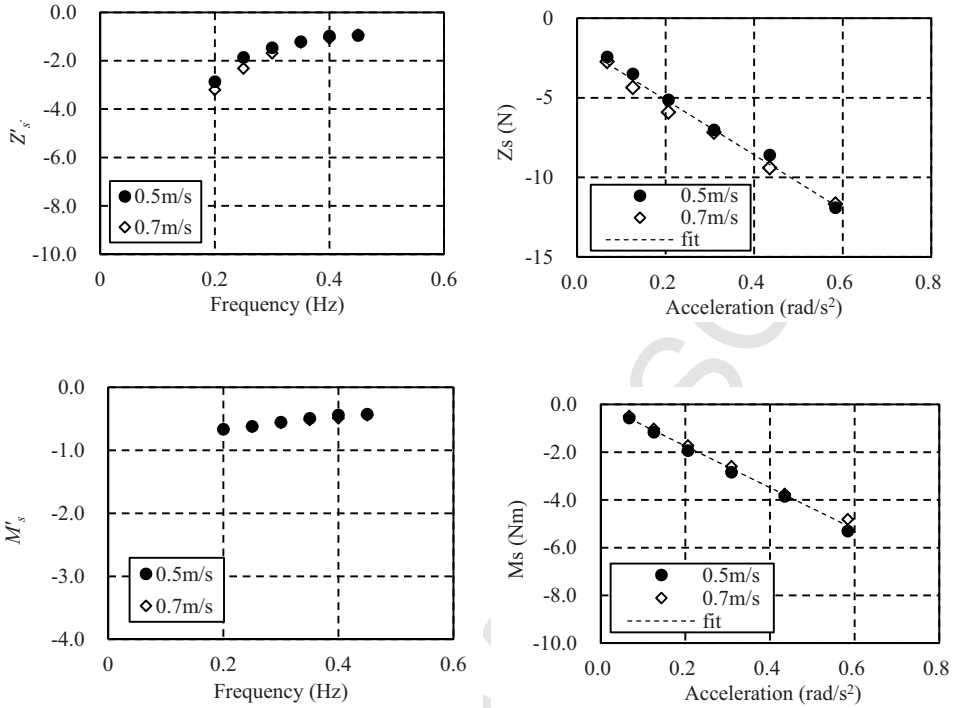

Fig 8 Inertial force and moment in purely pitching tests

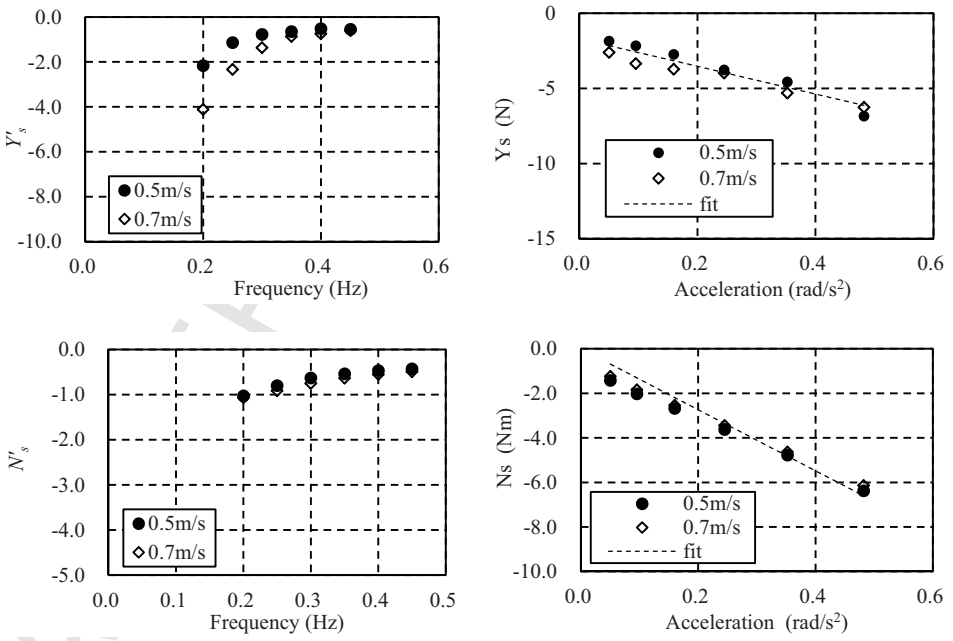

Fig 9 Inertial force and moment in purely yawing test

Table 4 Inertial hydrodynamic coefficients for pitching and yawing tests

set flow velocity (m/s)	real flow velocity (m/s)	$Z_{\dot{q}}$ (kg·m)	$M_{\dot{q}}$ (kg·m^2)	$Y_{\dot{r}}$ (kg·m)	$N_{\dot{r}}$ (kg·m^2)
0.5	0.532	-17.9	-4.49	-9.63	-5.88
0.7	0.751	-16.7	-5.96	-8.76	-5.31
average		-17.3	-5.22	-9.20	-5.60
set flow velocity (m/s)	real flow velocity (m/s)	$Z'_{\dot{q}} \times 10^2$ $\left(Z'_{\dot{q}} = Z_{\dot{q}}/\frac{1}{2}\rho l^4\right)$	$M'_{\dot{q}} \times 10^2$ $\left(M'_{\dot{q}} = M_{\dot{q}}/\frac{1}{2}\rho l^5\right)$	$Y'_{\dot{r}} \times 10^2$ $\left(Y'_{\dot{r}} = Y_{\dot{r}}/\frac{1}{2}\rho l^4\right)$	$N'_{\dot{r}} \times 10^2$ $\left(N'_{\dot{r}} = N_{\dot{r}}/\frac{1}{2}\rho l^5\right)$
0.5	0.532	-6.01	-1.75	-3.29	-2.29
0.7	0.751	-5.71	-2.32	-2.99	-2.07
average		-5.90	-2.04	-3.14	-2.18

4.2 Comparison and discussion of cross inertial coefficients

As well known, its inertial hydrodynamic matrix (Eq. (5)) for a rigid body is symmetric according to the potential theory. In other words, $Z_{\dot{q}}$ and $M_{\dot{w}}$ as well as $Y_{\dot{r}}$ and $N_{\dot{v}}$ should be the same, respectively. The fitted dimensionless coefficients based on the measured data compared in Table 5. It may be interesting to see that the magnitude of $Z'_{\dot{q}}$ is more than double that of $M'_{\dot{w}}$ while $Y'_{\dot{r}}$ and $N'_{\dot{v}}$ is not very much different from each other. The difference means that they are not as assumed by the potential theory. This is attributed to the existence of viscosity in real water and the complex nature of the structure of the ROV. As has been seen in Fig. 1, the ROV model is composed of many slender structural members orientating to different directions: horizontal, vertical or declined. The local added mass due to them can be significantly

affected by the viscosity as well known in offshore engineering, which may contribute to the non-symmetricity of the cross initial coefficients. The top-bottom and rea-front asymmetric shape of the ROV may also cause the different behaviors of boundary separation when the ROV oscillates in different directions and contribute to the non-symmetricity as well.

It is also interesting to see from Table 2 and Table 4 that the inertial coefficient for pitch due to heave has a value (cross inertial coefficients -$M_{\dot{w}}$) larger than the inertial coefficient for pitch due to pitch (main inertial coefficients $M_{\dot{q}}$). The inertial coefficient for heave due to pitch ($Z_{\dot{q}}$) has a considerable value but it is much smaller (~20%) than the inertial coefficient for heave due to heave ($Z_{\dot{w}}$). Comparing Table 3 and Table 4, one also finds that the term $N_{\dot{v}}$ is slightly larger than $N_{\dot{r}}$ while $Y_{\dot{r}}$ is much smaller than $Y_{\dot{v}}$. The descriptions and discussions in this and previous paragraphs reveal that the corresponding cross inertial coefficients can be very different (unlike what is derived by the potential theory) and that some cross inertial coefficients may not be negligible.

Table 5 Comparison of inertial coefficients

$Z'_{\dot{q}}$	$M'_{\dot{w}}$	$\lvert Z'_{\dot{q}}/M'_{\dot{w}}\rvert$	$Y'_{\dot{r}}$	$N'_{\dot{v}}$	$\lvert Y'_{\dot{r}}/N'_{\dot{v}}\rvert$
-5.90× 10^{-2}	-2.80× 10^{-2}	2.11	-3.14× 10^{-2}	-2.50× 10^{-2}	1.26

5. Conclusions

This paper presents an experimental study on the inertial hydrodynamic behaviors of a ROV. For this purpose, a series of model tests on a ROV model have been carried out in the circulating water channel in Harbin Engineering University. Its oscillations in heave, sway, pitch and yaw directions are generated by using a vertical planar motion mechanism (VPMM). The measured data are analyzed by using two data identification approaches: directly fitting the total forces (moments) measured or separating the inertial forces (moments) before fitting them. They can give similar results.

The resulting data shows that the magnitudes of the inertial forces and moments behaves linearly with the change of acceleration amplitudes. The fitting curves based on the obtained inertial coefficients agree well with the measured data and the corresponding formulae can be used for simulating the motions of the

ROV. In addition, the cross inertial coefficients are not equal to each other, e.g., $Z'_{\dot{q}}$ (inertial vertical forces coefficient induced by the pitching) is more than twice of $M'_{\dot{w}}$ (inertial pitch moment coefficients induced by heaving), though they should be the same according to the potential theory. It is also found that some cross inertial coefficients can be as large as or even larger than the corresponding main coefficients, indicating that one should not ignore the cross inertial coefficients for the ROV discussed in this paper. These findings may offer a sound reference not only for this ROV but also for others with asymmetrical shapes. In addition, it is hoped that the data provided in this paper may be used for validating numerical methods based on computational fluid dynamics in the cases involving the interaction between fluids and structures with complex geometry.

It is noted that the tests on the oscillation in surge direction is not carried out due to the restriction of experimental facility available.

Acknowledgements

This project is supported by the National Natural Science Foundation of China (Grant no.51579051 and no.51579056). The second author wishes to thank the Chang Jiang Visiting Chair professorship of Chinese Ministry of Education, supported and hosted by the HEU.

References

[1] F.A. Azis, M.S.M. Aras, M.Z.A Rashid, M.N. Othman, S.S. Abdullah, Problem Identification for Underwater Remotely Operated Vehicle (ROV): A Case Study. Procedia Engineering 41 (2012) 554-560.

[2] A. Smallwood, Advances in dynamical modeling and control of underwater robotic vehicles. PHD Thesis The Johns Hopkins University. Baltimore. Maryland. (2003).

[3] D.A. Smallwood, L.L. Whitcomb, Adaptive identification of dynamically positioned under water robotic vehicles. IEEE Trans. Control Syst. Technol. 11.4 (2003) 505–515.

[4] Y. Zhang, G.H. Xu, X.L. Xu, Measurement of the hydrodynamics coefficients of the microminiature open-shelf underwater vehicle. Shipbuilding of China 51.1 (2010) 63-72. (In Chinese)

[5] C. Chin, M. Lau, Modeling and testing of hydrodynamic damping model for a complex-shaped remotely-operated vehicle for control. Journal of Marine Science and Application 11.2 (2012) 150-163.

[6] Z.L. Lin, S.J. Liao, Calculation of added mass coefficients of 3D complicated underwater bodies by FMBEM. Communications in Nonlinear Science and Numerical Simulation 16.1 (2011) 187-194.

[7] H.H. Chen, H.H. Chang, C.H. Chou, P.H. Tseng, Identification of hydrodynamic parameters for a remotely operated vehicle using projective mapping method. Symposium on Underwater Technology and Workshop on Scientific Use of Submarine Cables and Related Technologies, 2007, pp. 427-436.

[8] J.J. Avila, K. Nishimoto, C.M. Sampaio, J.C. Adamowski, Experimental investigation of the hydrodynamic coefficients of a remotely operated vehicle using a planar motion mechanism. Journal of Offshore Mechanics and Arctic Engineering 134.2 (2012) 021601.

[9] J.P.J. Avila, J.C. Adamowski, Experimental evaluation of the hydrodynamic coefficients of a ROV through Morison's equation. Ocean Engineering 38.17 (2011) 2162-2170.

[10] J.P.J. Avila, D.C. Donha, J.C. Adamowski, Experimental model identification of open-frame underwater vehicles 60 (2013) 81-94.

[11]M. Nomoto, M. Hattori, A deep ROV ''Dolphin3K'': Design and performance analysis. IEEE J. Oceanic Eng. 11.3 (1986) 373–391.

[12] S.B. Fan, L. Lian, P. Ren, Research on Hydrodynamics Model Test for Deepsea Open -Framed Remotely Operated Vehicle. China Ocean Engineering 26 (2012) 329-339.

[13] Y.H. Eng, W.S. Lau, E. Low, G.G.L. Seet, C.S. Chin, A novel method to determine the hydrodynamic coefficients of an eyeball ROV, in: IAENG TRANSACTIONS ON ENGINEERING TECHNOLOGIES VOLUME I: Special Edition of the International Multi Conference of Engineers and Computer Scientists, vol. 1089, no. 1, 2009, pp. 11-22.

[14] Y.H. Eng, C.S. Chin, M.W.S. Lau, Added mass computation for control of an open-frame remotely-operated vehicle: application using WAMIT and MATLAB. Journal of Marine Science and Technology 22.2 (2013) 1-14.

[15] R. Yang, B. Clement, A. Mansour, M. Li, N. Wu, Modeling of a Complex-Shaped Underwater Vehicle for Robust Control Scheme. Journal of Intelligent and Robotic Systems: Theory and Applications, 80.3-4 (2015) 491-506.

[16] S.M.D, Work class ROV systems. http://www.smdusa.com/products/work-class-rov-systems/quantum.htm

[17] T.I. Fossen, Handbook of marine craft hydrodynamics and motion control. John Wiley & Sons 2011.

[18] E.M. Lewandowski, The dynamics of marine craft: maneuvering and seakeeping. Vol. 22. World scientific 2004.

[19] S. J. Xu, D.F. Han, Q.W. Ma, Hydrodynamic forces and moments acting on a remotely operate vehicle with an asymmetric shape moving in a vertical plane. European Journal of Mechanics-B/Fluids 54 (2015) 1-9.

Novelty of this paper

Providing experimental hydrodynamic inertial coefficients of an open-frame ROV;

Magnitudes of the inertial forces and moments behaves linearly with the change of acceleration amplitudes.

Cross inertial coefficients are not equal to each other or the added mass matrix is not symmetric.

Some cross inertial coefficients should not be ignored.